

# Incorporating Network Pharmacology and Experimental Validation to Identify Bioactive Compounds and Potential Mechanisms of Digitalis in Treating Anaplastic Thyroid Cancer

Lei Zhu, Ruimin Liang, Yawen Guo, Yefeng Cai, Fahuan Song, Yiqun Hu, Yunye Liu, Minghua Ge,\* and Guowan Zheng\*



Cite This: *ACS Omega* 2024, 9, 15590–15602



Read Online

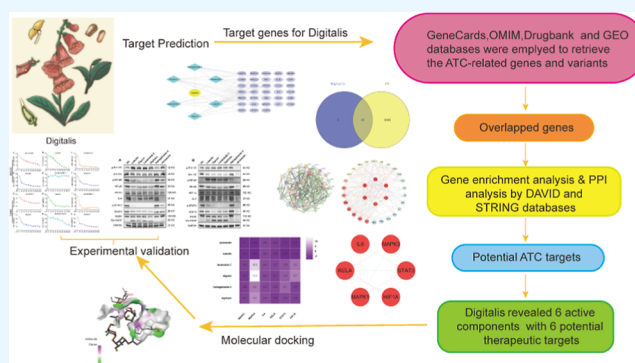
ACCESS |

Metrics & More

Article Recommendations

Supporting Information

**ABSTRACT:** Anaplastic thyroid cancer (ATC) is one of the most lethal malignant tumors for which there is no effective treatment. There are an increasing number of studies on herbal medicine Digitalis and its active ingredients for treating heart failure and arrhythmias have been revealed to have significant antitumor efficacy against a wide range of malignant tumors. However, the main components of Digitalis and the molecular mechanisms of its anti-ATC effects have not been extensively studied. Here, we screened the main components and core targets of Digitalis and verified the relationship between the active components and targets through network pharmacology, molecular docking, and experimental validation. These experiments showed that the active ingredients of Digitalis inhibit ATC cell activity and lead to ATC cell death through the apoptotic pathway.



## 1. INTRODUCTION

Thyroid cancer is the most common malignant tumor in the endocrine system. Recently, its incidence has increased rapidly and is predicted to become the fourth most common form of malignant tumor worldwide.<sup>1</sup> Thyroid cancer can be divided into four main subtypes: papillary thyroid cancer (PTC), follicular thyroid cancer (FTC), medullary thyroid cancer (MTC), and anaplastic thyroid cancer (ATC). Although most of thyroid cancers are PTC, which has low malignancy and a good prognosis,<sup>2</sup> the incidence of ATC, a highly aggressive tumor with a poor prognosis, is also increasing yearly.<sup>3</sup> The median survival time for patients with ATC is only 3.16 months, accounting for 40% of all thyroid cancer deaths.<sup>4</sup> Treatments for ATC, such as radiation therapy, chemotherapy, and radical surgery, have been employed,<sup>5</sup> but their efficacy is limited. Despite recent advances in targeted therapies and immunotherapy and FDA approval of the combination of the BRAF inhibitor dabrafenib and MEK inhibitor trametinib to treat ATC, only limited improvements in survival have been reported.<sup>6</sup> Thus, ATC remains one of the most lethal malignant tumors and no effective treatment is currently available.

The use of Chinese herbs for treating ATC has recently increased.<sup>7,8</sup> Digitalis has been employed for centuries to treat heart failure and arrhythmias and remains one of the most effective medications. Recent findings have suggested that the Digitalis extract has significant antitumor efficacy against

various malignant tumors, including cholangiocarcinoma, lung cancer, cervical cancer, pancreatic cancer, and multiple myeloma.<sup>9–13</sup> However, the main components of Digitalis and the molecular mechanisms by which it inhibits ATC are poorly understood.

Unlike conventional drugs, botanical drugs contain multiple active ingredients and can target multiple therapeutic pathways. For ATC treatment, it is crucial to identify key targets in the mechanism of action of Digitalis. Network pharmacology-grounded in systems biology and the network analysis of biological systems-focuses on selecting specific signaling nodes for drug design to target multiple targets.<sup>14</sup> Researchers have utilized network pharmacology to discover active compounds in drugs and traditional Chinese medicine (TCM), analyze drug combination laws and formula pairings, and elucidate the overall mechanisms of action.<sup>15,16</sup> This approach combines the roles of target and effector molecules and can accurately predict the therapeutic efficacy and mechanism of action of drugs.<sup>17</sup> Therefore, this study aimed to examine the core

Received: January 15, 2024

Revised: March 5, 2024

Accepted: March 8, 2024

Published: March 20, 2024



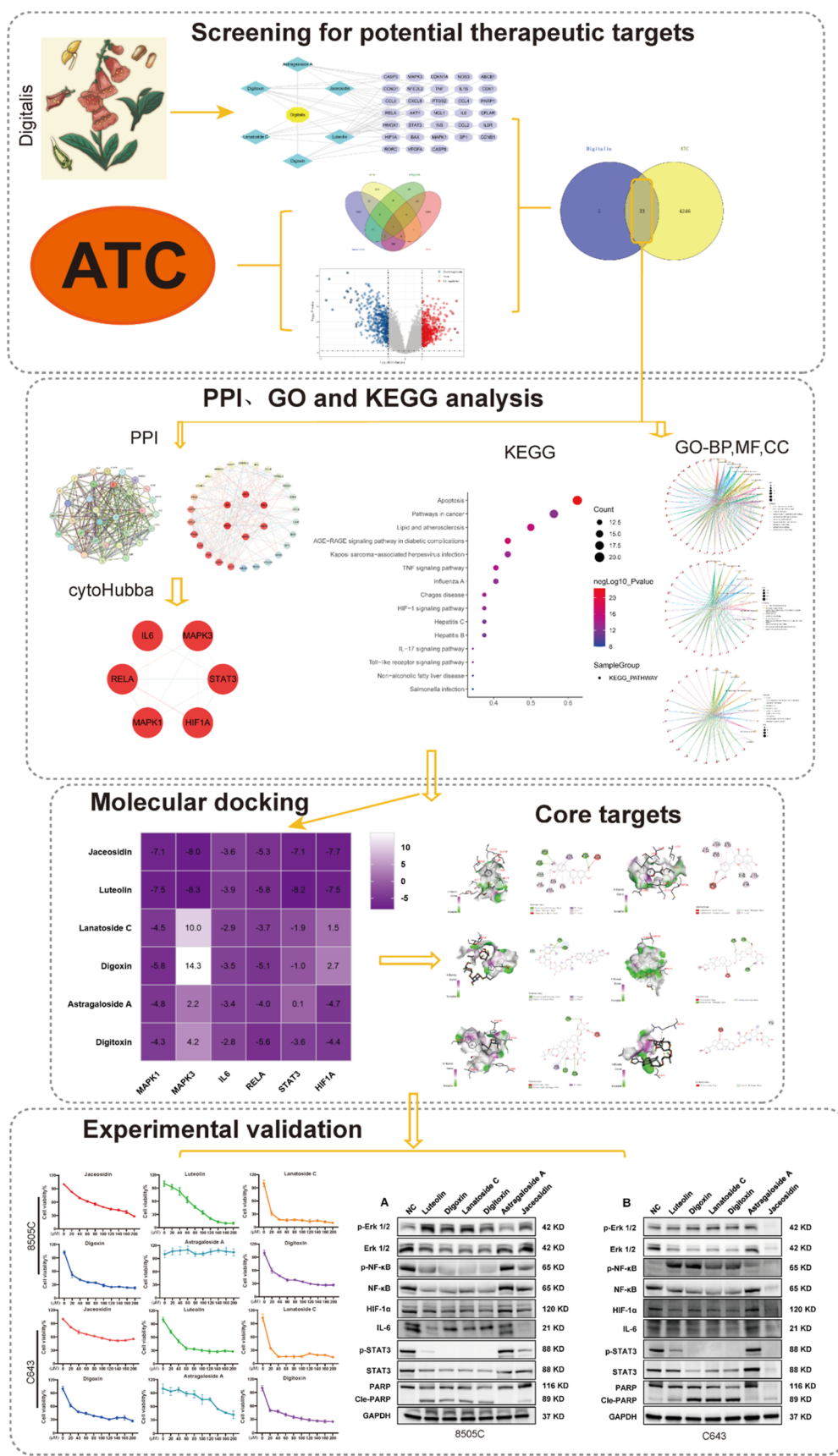


Figure 1. Flowchart.

targets, biological processes, and potential mechanisms of action of Digitalis in treating ATC using network pharmacol-

ogy. Our work will facilitate the screening of ATC drugs, elucidate the mechanism of action of Digitalis, and provide a

valuable reference for other medicinal plants as potential treatments for ATC. A flowchart of this study is displayed in Figure 1.

## 2. MATERIALS AND METHODS

No unexpected or unusually high safety hazards were encountered.

**2.1. Investigation of the Active Components and Targets of Digitalis.** The Traditional Chinese Medicine Systems Pharmacology (TCMSP)<sup>18</sup> is an online platform for web-based herbal pharmacology that encompasses the relationships between drugs, diseases, and targets.<sup>19</sup> Utilizing the TCMSP database, we searched for herbal ingredients and screened for active components of Digitalis, defined by the criteria of an active molecule (DL)  $\geq 0.18$ , indicating better pharmacological activity and oral bioavailability (OB)  $\geq 30\%$ .<sup>20,21</sup> We also consulted TCMSP for the protein targets of these screened active ingredients and supplemented their chemical composition and targets from the literature in CNKI and PubMed. In the UniProt database<sup>22</sup> (<http://www.uniprot.org>), the protein targets were normalized using the species “*Homo sapiens*”. Subsequently, a network of relationships between active ingredients and targets was built using Cytoscape 3.7.2.<sup>23</sup>

**2.2. Target Collection Related to ATC.** Potential therapeutic targets of ATC were identified using GeneCards<sup>24</sup> (<http://www.genecards.org/>), OMIM<sup>25</sup> (<https://omim.org/>), and DrugBank<sup>26</sup> (<https://go.drugbank.com/>) databases. Microarrays related to ATC were retrieved from the Gene Expression Omnibus (GEO) database using “anaplastic thyroid cancer” as the keyword and “*H. sapiens*” as the species. Differentially expressed genes (DEGs) between ATC patients and the normal population were identified using the R software Limma package, with the selection criteria set at  $\log_{2}FCI > 1$  and  $P < 0.05$ .<sup>27</sup> Data were visualized through volcano plots and heatmaps using the R packages ggplot2 and pheatmap.<sup>28</sup> Using the UniProt database, disease targets and potential drug target symbols were normalized. Venny 2.1 was used to identify genes associated with ATC,<sup>29</sup> and these overlaps were then cross-referenced with the targets of Digitalis’ active ingredients as potential targets for ATC intervention.

**2.3. Network Construction for Protein–Protein Interaction.** Based on the String database<sup>30</sup> (<https://cn.string-db.org>), a PPI network was created using the gene for the interaction between Digitalis and ATC as the core gene, with “*H. sapiens*” as the species and a confidence level of  $>0.9$ . The PPI network was visualized and analyzed using the Cytoscape software.<sup>31</sup> The Cytohubba plugin in Cytoscape was employed to analyze the topological characteristics of the targets in the network, demonstrated using the MCC algorithm based on key topological parameters, such as degree and betweenness centrality, and listing the top 20 nodes based on the degree value. The key modules in the PPI network were then further analyzed using the MCODE plugin in terms of degree centrality, betweenness centrality, and closeness centrality exceeding the median to filter out the hub genes.

**2.4. Pathway Enrichment Analyses Based on GO and KEGG Data.** DAVID 6.8 was used to perform GO and KEGG analyses,<sup>32</sup> examining molecular function (MF), biological process (BP), cellular component (CC), and key signaling pathways to reveal the underlying mechanisms.

**2.5. Docking of Molecules.** Compound structures were downloaded from the PubChem platform ([https://pubchem.](https://pubchem.ncbi.nlm.nih.gov/)

[ncbi.nlm.nih.gov/](https://pubchem.ncbi.nlm.nih.gov/)) and converted into Mol2 format files using Chem3D software. The protein structures were downloaded from the RCSB Web site (<https://www.rcsb.org/>). The AutoDock Vina software was employed to add hydrogen and remove water molecules and ligands.<sup>23</sup> The final visualization was created using AutoDock Vina and Discovery Studio 2020 based on molecular and conformational docking,<sup>33</sup> respectively.

**2.6. Culture of Cells and Cell Lines.** The ATC cell line 8505C was obtained from the German Collection of Microorganisms and Cell Cultures (DSMZ), whereas the National Infrastructure of Cell Line Resource (Shanghai, China) provided the C643 cell line. The cells were cultured in RPMI 1640 medium (HyClone, Logan, UT, United States) containing 10% fetal bovine serum (Serana Europe GmbH, Brandenburg, Germany) and 1% penicillin/streptomycin (Cienry Biotech, China). The cultures were maintained at 37 °C in a 5% CO<sub>2</sub> incubator.

**2.7. Cell Viability Assay.** CCK-8 colorimetry (Yeason Biotech, Shanghai, China) was utilized to assess the effects of various active components of Digitalis on the ATC cell activity. Cells of the 8505C and C643 lines (5000/well) were inoculated in 96-well plates and incubated for 24 h before being treated with different concentrations of the active ingredients (Jaceosidin, Luteolin, Lanatoside C, Digoxin, Digitoxin, and Astragaloside A) for another 24 h. The main active ingredients were supplied by TargetMol (USA). Cell viability was determined using the CCK-8 colorimetric assay.

**2.8. Western Blotting.** Cells ( $1.5 \times 10^6$ /well) of the 8505C and C643 lines were cultured in 6-well plates for 24 h. Afterward, the cells were treated with the main active ingredients (Jaceosidin, Luteolin, Lanatoside C, Digoxin, Digitoxin, and Astragaloside A) at their IC<sub>50</sub> values for 24 h. Proteins were extracted using PMSF-containing Western and IP lysis buffers (Beyotime Biotech, Shanghai, China). Equal amounts of protein (20  $\mu$ g) were loaded into each lane of a Precast Protein Plus Gel, 4–20% (Yeason Biotech, Shanghai, China), separated by electrophoresis, and then transferred to a polyvinylidene fluoride (PVDF) membrane. The membrane was blocked with TBST containing 1% Tween-20 and 5% skimmed milk for 1.5 h and then incubated overnight at 4 °C with primary antibodies. Erk1/2 (1:2000, Cell Signaling Technology, Danvers, MA, USA), p-Erk1/2 (1:2000, Cell Signaling Technology, Danvers, MA, USA), NF- $\kappa$ B (1:1000, Cell Signaling Technology, Danvers, MA, USA), p-NF- $\kappa$ B (1:1000, Cell Signaling Technology, Danvers, MA, USA), HIF-1 $\alpha$  (1:1000, Cell Signaling Technology, Danvers, MA, USA), IL-6 (1:1000, Cell Signaling Technology, Danvers, MA, USA), STAT3 (1:1000, HUABIO, Hangzhou, China), p-STAT3 (1:1000, Abcam, Cambridge, MA, USA), PARP (1:1000, Proteintech, Wuhan, China), and GAPDH (1:5000, Proteintech, Wuhan, China) were used as primary antibodies. An HRP-linked secondary antibody solution (antimouse or antirabbit IgG, 1:3000, Beyotime Biotech, Shanghai, China) was applied for 1 h. The membranes were analyzed using the FDBioDura ECL kit (FDBio Science, China) and imaged using an Invitrogen iBright imager (Thermo Fisher Scientific, Invitrogen, USA). Band density was quantified using the ImageJ software.

**2.9. Analyses of Statistics.** Statistical analyses were performed using the GraphPad Prism 9.5 software. All values are expressed as mean  $\pm$  standard deviation (SD). A  $P$ -value of  $<0.05$  was considered statistically significant.



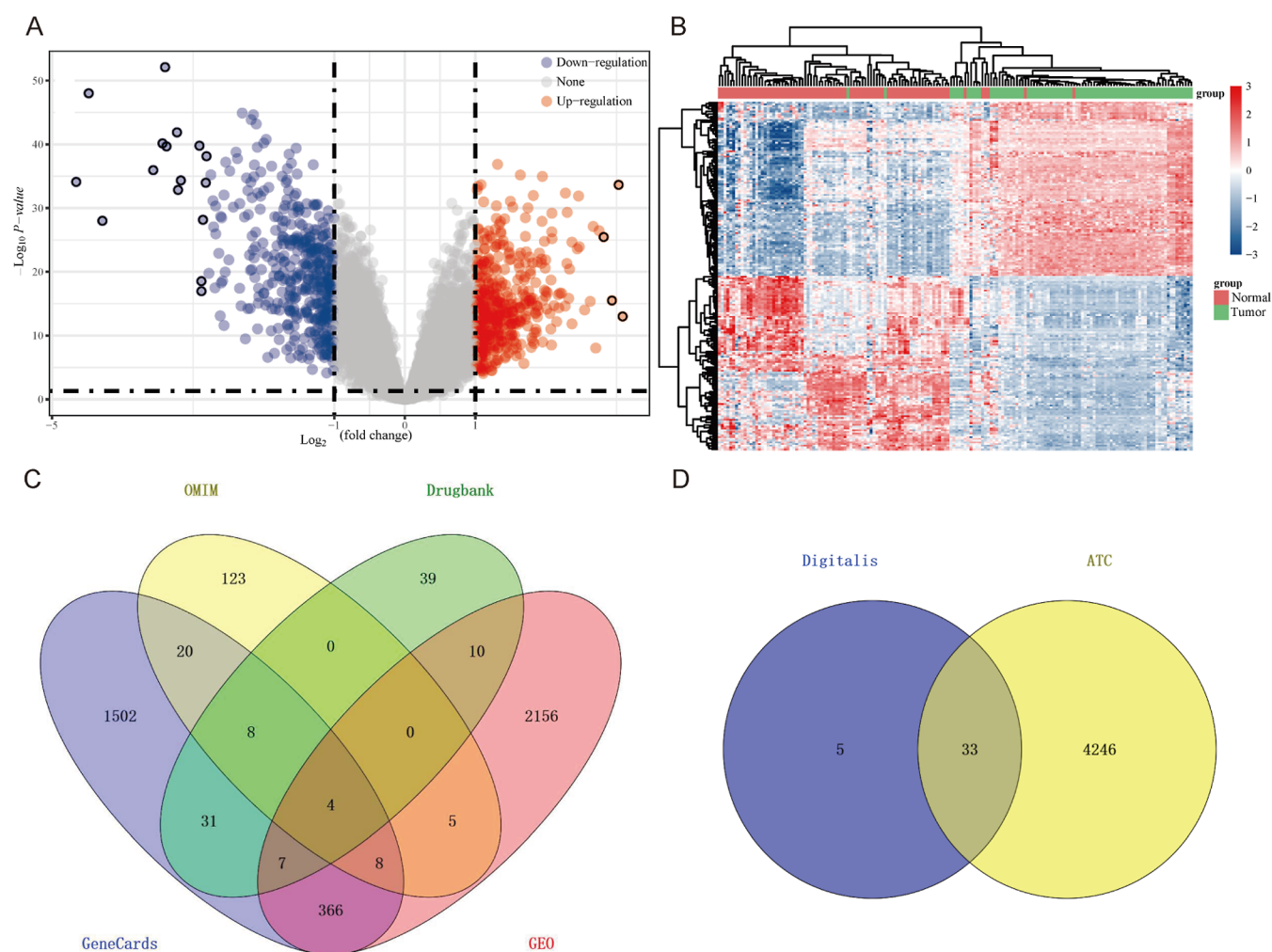


**Figure 2.** Volcano plot (A) and heat map (B) of DEGs between ATC samples and normal thyroid samples in GEO database (contains GSE29265, GSE76039, and GSE33630 data sets). (C) Venn diagram of ATC-related targets in six disease databases and the GEO database. (D) Venn diagram demonstrating the number of overlapping genes between Digitalis and ATC.

### 3. RESULTS

**3.1. Digitalis Active Ingredients and Targets of Action.** Ten active ingredients of Digitalis were obtained from the TCM and active ingredient databases (Table S1), with the SMILES of each ingredient acquired. The targets corresponding to each ingredient, i.e., Digitalis ingredient targets, were identified by inputting SMILES into TargetNet. In total, 52 targets were associated with the 10 active ingredients (Table S2). Volcano and heatmaps of DEGs were sourced from three data sets (GSE29265, GSE76039, and GSE33630) from the GEO database, yielding 2557 DEGs between ATC and normal tissues (Table S3), with 1430 downregulated and 1127 upregulated DEGs (Figure 2A,B). Further analysis of the GeneCards, OMIM, and DrugBank databases yielded 1946, 168, and 101 thyroid cancer-related genes, respectively, resulting in 4279 unique genes after eliminating of duplicates (Figure 2C). By intersecting the targets of Digitalis components with thyroid cancer differential genes, we identified 33 common targets (Figure 2D). Six active ingredients correspond to these common targets, as demonstrated in Table 1. An herbal component-target network diagram (H–C–T) was constructed using Cytoscape v3.7.2 to visualize the complex relationships (Figure 3).

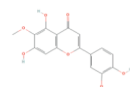
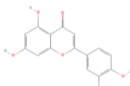
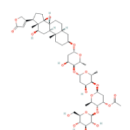
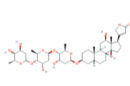
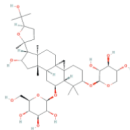
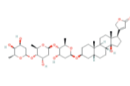
**3.2. PPI Network Construction and Analysis.** Of the 33 targets found between ATC and the active ingredients of Digitalis, a PPI network was constructed based on the STRING database (Figure 4A). By analyzing the topological features of protein–protein interactions using Cytoscape v3.7.2, the top 20 targets were ranked by degree (Figure 4B). Within the CytoHubba plugin, the top six hub genes (STAT3, MAPK1, MAPK3, IL6, RELA, and HIF1A) were identified by using the MCC algorithm (Figure 4D), revealing a core network with 40 nodes and 52 edges (Figure 4C).

**3.3. Analyses of GO Functional Enrichment.** To elucidate the biological characteristics of the 33 shared target genes, GO enrichment analysis was conducted using DAVID 6.8. We selected enrichment results with a  $P$ -value  $< 0.01$ , a minimum overlap of 3, and a minimum fold enrichment of 1.5. Figure 5A–C displays the top 10 terms significantly enriched for MF, BP, and CC. Several BPs—such as apoptotic signaling pathways, negative regulation of apoptosis, and response to oxidative stress—closely linked to ATC development—were among the top 10 identified. These findings suggest that Digitalis may exert its anticancer effects through these biological processes.

**3.4. Analyses of KEGG Functional Enrichment.** Based on KEGG pathway analysis with a threshold of  $P < 0.01$ , we



Table 1. Six Core Ingredients of Digitalis

No.	Ingredient	PubChem CID	Molecular Formula	Molecular Weight	2D Structure
1	Jaceosidin	5379096	C <sub>17</sub> H <sub>14</sub> O <sub>7</sub>	330.29	
2	Luteolin	5280445	C <sub>15</sub> H <sub>10</sub> O <sub>6</sub>	286.24	
3	Lanatoside C	656630	C <sub>49</sub> H <sub>76</sub> O <sub>20</sub>	985.1	
4	Digoxin	2724385	C <sub>41</sub> H <sub>64</sub> O <sub>14</sub>	780.9	
5	Astragaloside A	13943299	C <sub>41</sub> H <sub>68</sub> O <sub>14</sub>	785	
6	Digitoxin	441207	C <sub>41</sub> H <sub>64</sub> O <sub>13</sub>	764.9	

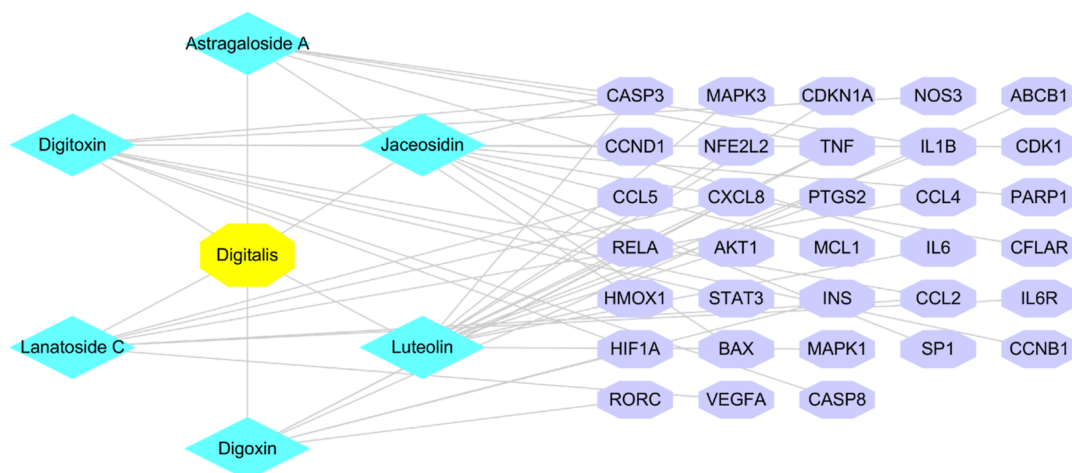


Figure 3. Network of the relationship between the active ingredients and the targets of Digitalis.

further investigated the role of the 33 overlapping target genes in ATC. The apoptosis pathway appeared at the top of the list in Figure 5D, suggesting that Digitalis may exert anti-ATC effects through the apoptosis pathway.

**3.5. Validation of Molecular Docking.** Following PPI network analysis and KEGG enrichment analysis, molecular docking was performed between the six core components (Jaceosidin, Luteolin, Lanatoside C, Digoxin, Digitoxin, and Astragaloside A) and the six key target proteins, which were screened from 33 target genes based on degree centrality, specific centrality, and proximity centrality over the median, namely, MAPK3, STAT3, MAPK1, HIF1A, RELA, and IL6. Docking affinity scores were calculated, as displayed in Figure 6A. The best docking interactions were observed in Jaceosidin with MAPK3, Luteolin with STAT3, Lanatoside C with

MAPK1, Digoxin with MAPK1, Astragaloside A with HIF1A, and Digitoxin with RELA (Figure 6B–G).

**3.6. Inhibitory Effect of These Six Active Ingredients on the Activity of ATC Cells.** The 8505C and C643 cells were treated with the six active ingredients (Jaceosidin, Luteolin, Lanatoside C, Digoxin, Astragaloside A, and Digitoxin) to test the effects of Digitalis. The results indicated that the primary components inhibited the ATC cell viability in a concentration-dependent manner. The 24 h IC<sub>50</sub> values against 8505C and C643 were 98.13, 89.31, 5.42, 53.01, >200, and 61.57 μM (Figure 7A–F), as well as 130.7, 31.43, 7.22, 47.63, 111.5, and 63.63 μM (Figure 7G–L), respectively.

**3.7. Six of the Active Ingredients Induced Apoptosis in ATC Cells.** The six active ingredients were administered to 8505C and C643 cells at their respective IC<sub>50</sub> concentrations

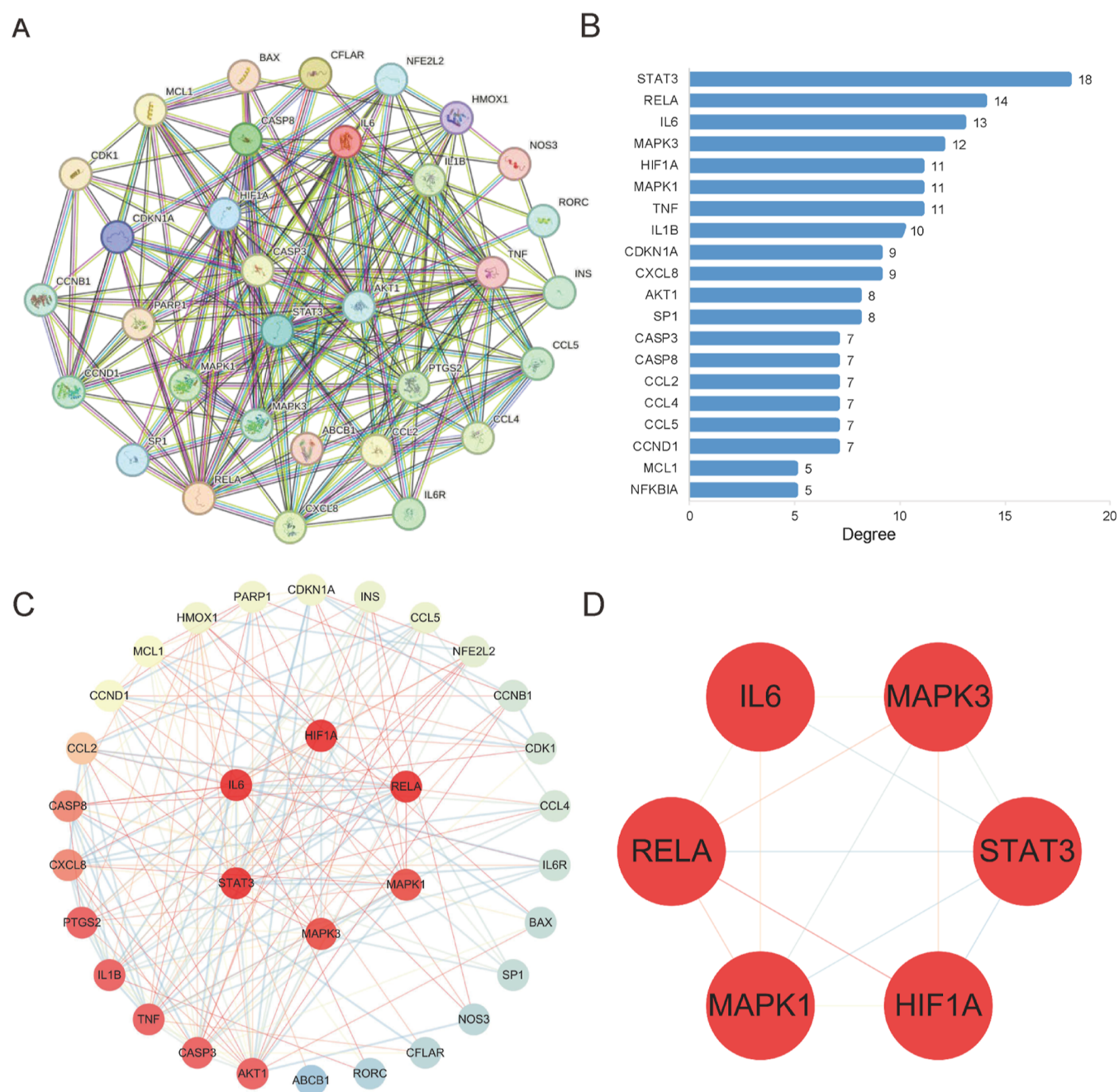


**Figure 4.** Results of the PPI network of the overlapping targets. (A) The PPI network of the overlapping targets. (B) Bar plot of the number of hub gene links. (C) Protein interaction core network. (D) The top six hub genes.

and incubated for 24 h. Based on the KEGG analysis and molecular docking results, we focused on the effects of the six active ingredients of Digitalis on the six core components (STAT3, MAPK1, MAPK3, IL6, RELA, and HIF1A). Western blotting results confirmed that most active ingredients of Digitalis were able to affect Erk1/2 (MAPK3/1), p-Erk1/2, NF- $\kappa$ B (RELA), p-NF- $\kappa$ B, STAT3, p-STAT3, IL-6, and HIF-1 $\alpha$ . The expressions of STAT3, p-STAT3, IL-6, NF- $\kappa$ B, Erk1/2, and HIF-1 $\alpha$  were downregulated in the two cell lines after the action of the active components of Digitalis, and the level of p-Erk1/2 expression was increased. The expression of these proteins showed a consistent trend in the two cell lines, but the trend of p-NF- $\kappa$ B was inconsistent between the two cell lines, possibly due to cellular heterogeneity. For p-STAT3 and p-NF-

$\kappa$ B, at least one of the proteins was downregulated in both cell lines. As previously mentioned in the CCK-8 assay, Astragaloside A did not have a significant effect on the two ATC cell lines. Therefore, in the Western blotting results, the changes in the above proteins were not significant after administration of Astragaloside A compared with the NC group, and these two results were consistent. In addition, Western blotting results confirmed that the active ingredients could induce cleavage of PARP, except Astragaloside A, leading to apoptosis in 8505C and C643 cells (Figure 8, quantitative charts in Figure S1).

#### 4. DISCUSSION

Globally, the incidence of thyroid cancer has continued to rise rapidly in many countries and regions over the past three

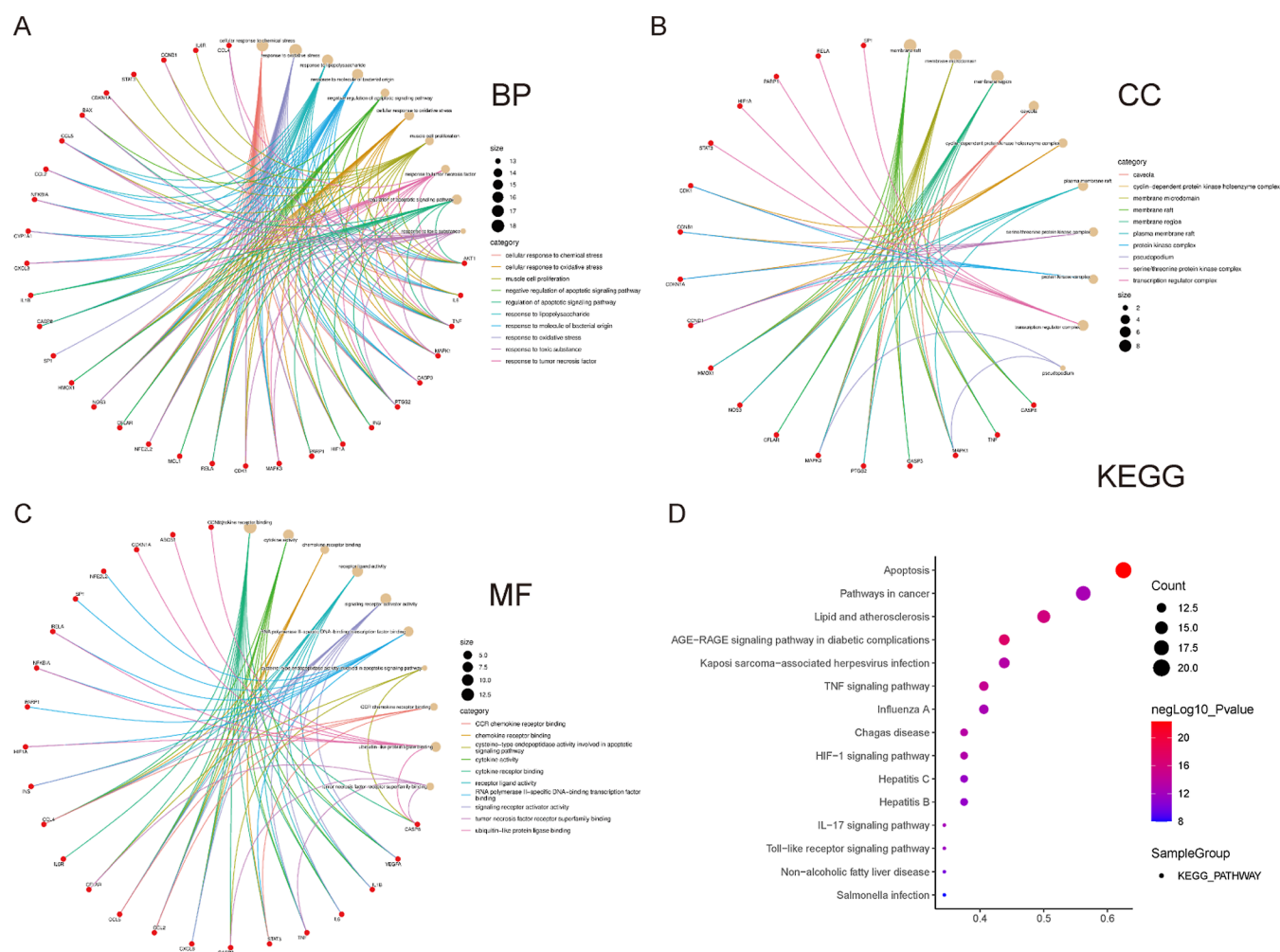


**Figure 5.** GO and KEGG enrichment analyses of Digitalis intervening ATC intersection targets. The top 10 terms of BP (A), CC (B), and MF (C) enrichment analysis of the GO enrichment analysis. (D) Bar chart of the top 10 KEGG pathways.

decades, making it the most common endocrine malignancy.<sup>34</sup> Papillary thyroid carcinoma (PTC) is the most prevalent type of thyroid cancer, whereas anaplastic thyroid carcinoma (ATC) accounts for only 1–2% of all thyroid cancers.<sup>35</sup> However, ATC is the least differentiated, leading to the highly aggressive and invasive behavior of ATC cells, resulting in a high degree of malignancy. This can include infiltration and metastasis at an early tumor stage, often with a disease course of less than 1 year from onset to death.<sup>36</sup> This malignancy poses a serious threat to human health and is currently resistant to effective treatment. An increasing number of studies on ATC, including targeted therapy,<sup>37,38</sup> immunotherapy,<sup>5,39</sup> nanomedicines,<sup>40</sup> and Chinese medicine therapy,<sup>7,8</sup> have shown encouraging results. Because herbal medicines and monomers have a wide range of sources, their research prospects for treating ATC are substantial. They can inhibit ATC tumor activity through apoptosis and antiangiogenesis<sup>41</sup> and induce mitochondrial apoptosis and cell-cycle arrest to inhibit ATC cells.<sup>8</sup> Notably, our group's previous research found that herbal monomers play an antitumor role by inducing pyroptosis and apoptosis in ATC cells.<sup>7</sup> However, there is no definitive proof of the effectiveness of herbal medicines and monomers for anti-ATC treatment.

With the recent advancement of computer technology and biomedicine, the theoretical study of network pharmacology

has matured, becoming an important tool for discovering and developing TCM, particularly for investigating its molecular activity. An integrated network model of cyberpharmacology incorporates multiple components, targets, and pathways, aligning with TCM's holistic approach and the complex nature of disease development. UniProt and TCMSP are two widely used databases in network pharmacological research that play an important role in capturing molecular interactions and pharmacological properties in herbal medicine research. UniProt is a comprehensive, rigorously audited protein sequence and annotation database that integrates data from several protein databases, such as Swiss-Prot, TrEMBL, and Pir, providing a one-stop platform for research. With reliable data quality, rich annotations, and cross-references to multiple databases, UniProt can assist researchers in identifying target proteins in herbal medicines and analyzing their functions and interactions.<sup>22</sup> The TCMSP is a database dedicated to the systemic pharmacological study of herbal medicines, which integrates information on various aspects such as herbal components, targets, and diseases. It also adopts advanced computational methods to predict the interactions between herbal components and targets and provides rich visualization tools. These tools can help quickly screen out the active ingredients in herbal medicines in the research and predict the interactions between them and their targets, providing



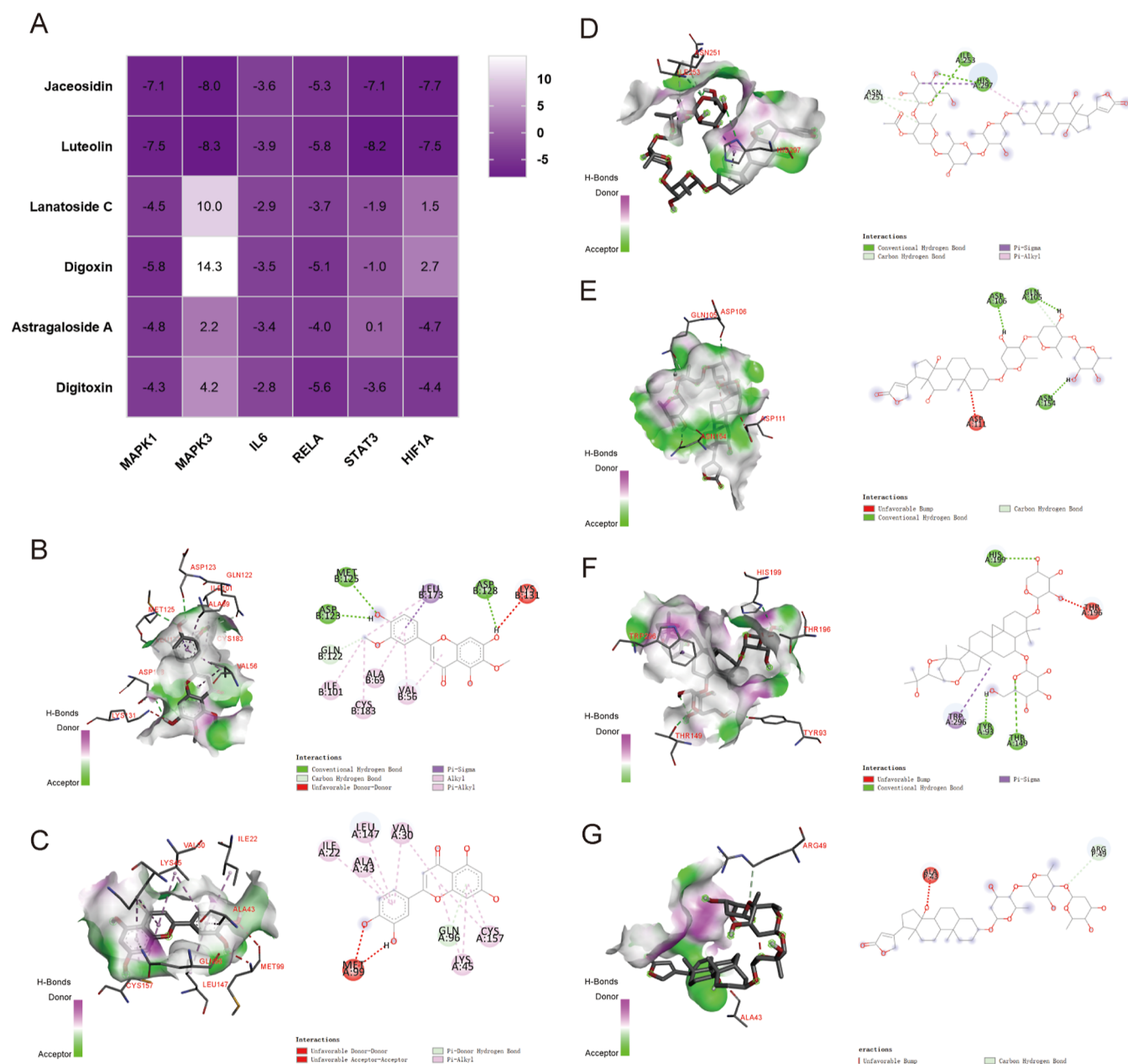


**Figure 6.** Results of molecular docking. (A) The heatmap of the docking score. Molecular docking results of (B) Jaceosidin and MAPK3, (C) Luteolin and STAT3, (D) LanatosideC and MAPK1, (E) Digoxin and MAPK1, (F) AstragalosideA and HIF1A, and (G) Digitoxin and RELA.

powerful support for investigating the pharmacological effects of herbal medicines.<sup>18</sup> In this study, network pharmacology, molecular docking experiments, and in vitro assays were combined to predict and validate the targets and mechanisms of action of Digitalis for treating ATC. We screened 10 active ingredients of Digitalis from a TCM database and identified 52 protein targets using the UniProt database. We then combined the differentially expressed genes of ATC with normal tissue data from three data sets (GSE29265, GSE76039, and GSE33630) sourced from the GeneCards, OMIM, and Drugbank databases with the GEO database to obtain 4279 genes. By intersecting the target genes of ATC and Digitalis, we identified 33 key genes that may be crucial for Digitalis resistance in ATC. Using these genes, we excluded the four less active components and identified the main active components of Digitalis (Jaceosidin, Luteolin, Lanatoside C, Digoxin,

Digitoxin, and Astragaloside A). Additionally, we constructed a PPI network to isolate the top 20 genes (STAT3, RELA, IL6, MAPK3, HIF1A, MAPK1, TNF, IL1 $\beta$ , CDKN1A, CXCL8, AKT1, SP1, CASP3, CASP8, CCL2, CCL4, CCL5, CCND1, MCL1, and NFKB1A) associated with ATC resistance in Digitalis and analyzed the key modules in the PPI network according to the criteria of degree centrality, median centrality, and closeness centrality over the median to obtain six core target genes (MAPK3, STAT3, MAPK1, HIF1A, RELA, and IL6). GO and KEGG analyses of the 33 key genes suggested that the apoptotic signaling pathway might be the most crucial for the anti-ATC effects of Digitalis.

The study found that Digitalis interferes with several ATC signaling pathways, particularly the MAPK pathway. In the eukaryotic signaling network, the MAPK pathway governs fundamental cellular processes such as differentiation, pro-

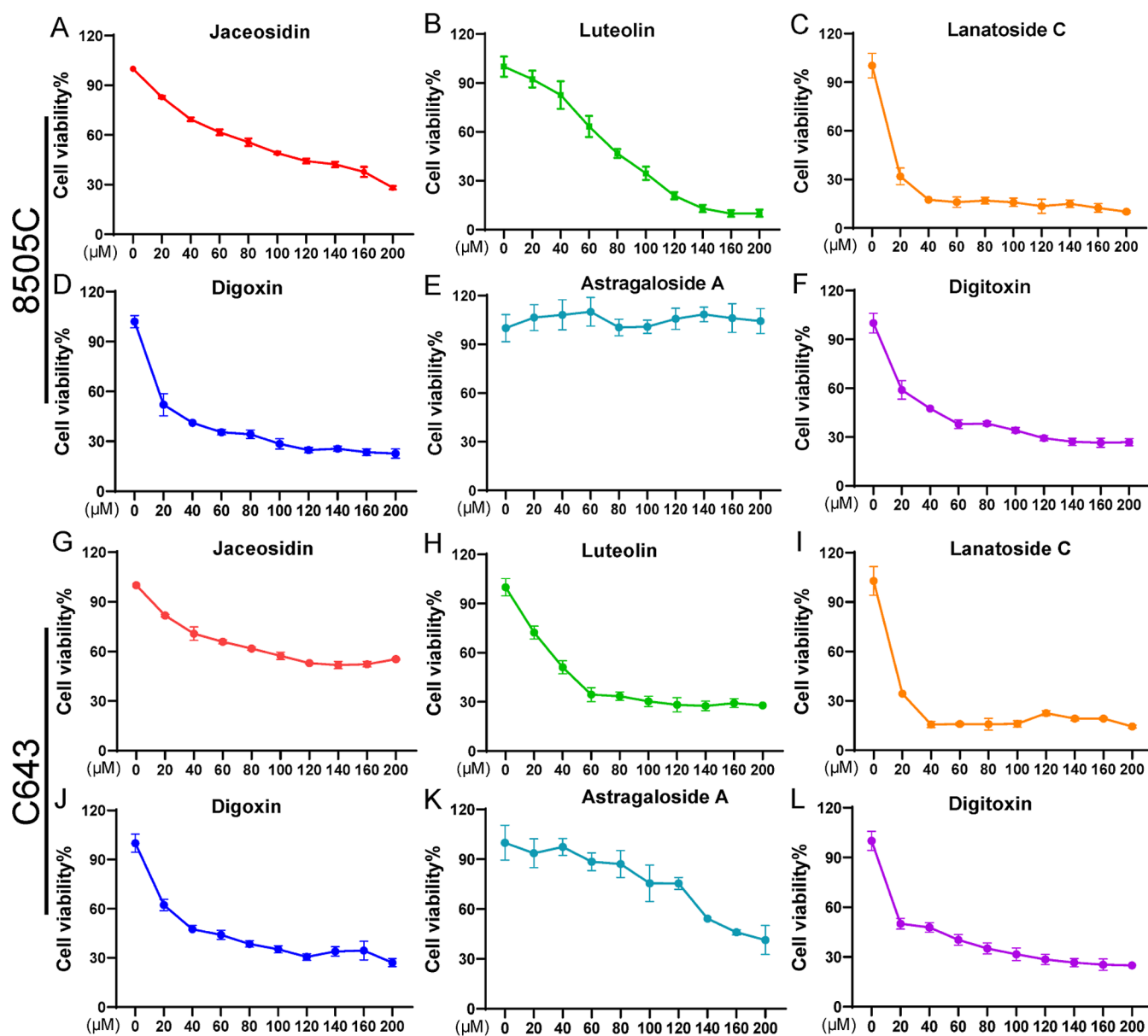


**Figure 7.** Cell viability inhibitory effects of six active compounds of Digitalis, including Jaceosidin (A), Luteolin (B), Lanatoside C (C), Digoxin (D), Digitoxin (E), and Astragaloside A (F) on 8505C cells. Cell viability inhibitory effects of six active compounds of Digitalis, including Jaceosidin (G), Luteolin (H), Lanatoside C (I), Digoxin (J), Digitoxin (K), and Astragaloside A (L) on C643 cells. Drug concentration–cell viability curves were generated based on the cell viability assay. All data were expressed as mean  $\pm$  SD ( $n = 6$ ).

liferation, and apoptosis.<sup>42,43</sup> The MAPK signaling cascade influences these cellular functions and is a primary target for pharmacological intervention, especially in oncology. Previous studies have demonstrated that mutations activating the MAPK signaling cascade, typically in BRAF or RAS oncogenes, primarily trigger thyroid cancer,<sup>44</sup> while ATC undergoes further genetic alterations to become more aggressive.<sup>45</sup> Currently, MAPK inhibitors, such as dabrafenib, trametinib, and simetinib, are used to treat advanced thyroid cancer,<sup>46</sup> with dabrafenib plus trametinib being FDA-approved specifically for ATC with BRAF mutations.<sup>47</sup> This underscores the significance of the MAPK signaling pathway in the ATC.

For further validation, we chose the hub genes (MAPK3, STAT3, MAPK1, HIF1A, RELA, and IL6) of ATC and the major active ingredients of Digitalis (Jaceosidin, Luteolin, Lanatoside C, Digoxin, Digitoxin, and Astragaloside A) for

molecular docking based on the PPI, GO, and KEGG network analyses. Molecular docking is a computational technique that predicts interactions between small molecules and proteins at the atomic level and has become an important element in computerized drug development. Molecular docking technology determines the affinity of the two parties by assessing the binding energy between the receptor and ligand, the geometric spatial matching between the receptor and ligand, the strength and number of chemical interactions between the receptor and ligand, and the effect of the physical properties of the receptor and ligand on the binding. It also evaluates the reliability of the docking results using the docking scores, root-mean-square deviations, and the free energies of binding as a function of the binding score.<sup>48,49</sup> In our study, AutoDock Vina was the fastest and most widely used open-source software for molecular docking. The results disclosed that the main active ingredients

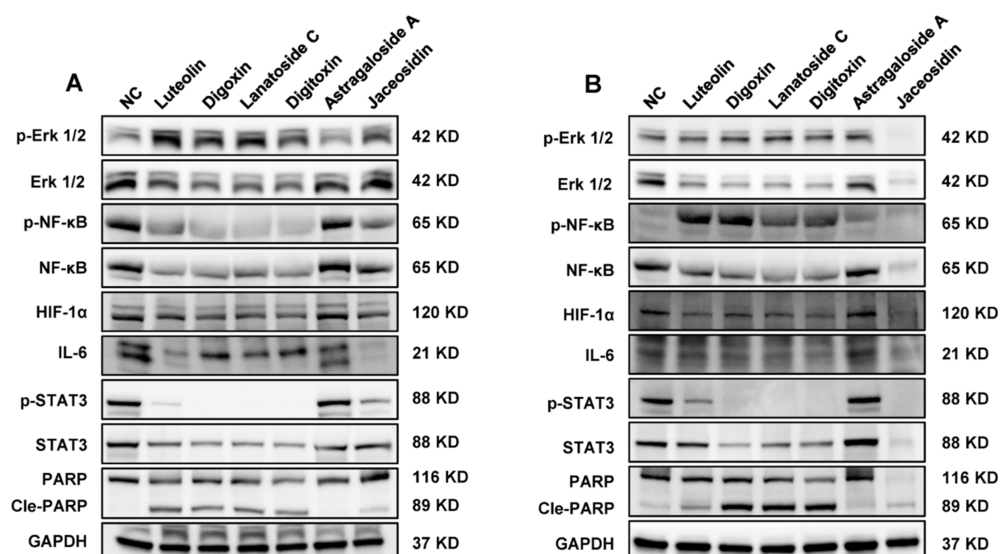


**Figure 8.** Representative profiles demonstrating apoptosis of the treatment with the main ingredients of Digitalis alone. The effect of the main ingredient components on six hub genes was observed and could decrease PARP expression in 8505C (A) and C643 (B).

had a high affinity for the target genes. The main active components of Digitalis suppressed ATC cell proliferation and induced apoptosis in a concentration-dependent manner, verifying the accuracy of the network analysis. These results provide a new theoretical basis for the ATC treatment.

There are various previous studies on these active ingredients. Studies have revealed that Jaceosidin is able to induce apoptosis in gastric cancer cells by regulating ROS-mediated signaling pathways<sup>50</sup> and is able to inhibit the progression and metastasis of NSCLC.<sup>51</sup> Luteolin performs various anticancer effects mainly by inhibiting proliferation and invasion, stimulating apoptosis, intercepting the cell cycle, regulating autophagy and immunity, inhibiting inflammatory responses, inducing iron death and pyroptosis, and epigenetic modifications.<sup>52</sup> Lanatoside C can target the ZDHHC21/FASN axis for treating diffuse large B-cell lymphoma<sup>53</sup> and can inhibit the proliferation of cholangiocarcinoma and promote apoptosis.<sup>9</sup> Digoxin can block the PI3K/Akt pathway to exert anticancer activity on human nonsmall cell lung cancer cells<sup>13</sup> and can also inhibit the proliferation, migration, and invasion of colorectal cancer cells.<sup>54</sup> Astragaloside A can inhibit the progression of colorectal cancer cells<sup>55</sup> and inhibit the migration and EMT progression of cervical cancer cells.<sup>56</sup> Digitoxin has an inhibitory effect on pancreatic cancer cells<sup>57</sup> and can reduce HIF-1 $\alpha$  and STAT3 to promote apoptosis and inhibit the proliferation and migration of KRAS mutant human colon cancer cells.<sup>58</sup> However, the effects of these active ingredients on thyroid cancer, especially undifferentiated thyroid cancer, have not yet been reported. Our study verified the anti-ATC effects of the active ingredients of digitalis through network pharmacology, molecular docking, and preliminary experiments. These results provide a new theoretical basis for ATC treatment. However, there are limitations to our study. Our study was only a preliminary result, and we did not explore the specific mechanism of the antitumor effect of these active ingredients in more depth. Therefore, our next step will be to delve deeper into the anti-ATC mechanisms of these active ingredients through further *in vivo* and *in vitro* experiments with the aim of enabling clinical translation.

## 5. CONCLUSIONS

In the present study, network pharmacology, molecular docking, and *in vitro* experiments were used to predict and validate the anti-ATC mechanism of action and the potential targets of the active constituents of Digitalis. Specifically, these active components inhibited ATC cell activity and induced cell death through an apoptotic pathway. Consequently, these active ingredients show promise as effective treatments for ATC.

## ■ ASSOCIATED CONTENT

### Supporting Information

The Supporting Information is available free of charge at <https://pubs.acs.org/doi/10.1021/acsomega.4c00373>.

Ten active ingredients of Digitalis; 52 targets for 10 active ingredients in Digitalis; DEGs between ATC and normal tissues; and quantitative charts (PDF)

## ■ AUTHOR INFORMATION

### Corresponding Authors

**Minghua Ge** – Suzhou Medical College of Soochow University, 215123 Suzhou, Jiangsu, China; Otolaryngology & Head and Neck Center, Cancer Center, Department of Head and Neck Surgery, Zhejiang Provincial People's Hospital, Affiliated People's Hospital, Hangzhou Medical College, 310014 Hangzhou, Zhejiang, China; Key Laboratory of Endocrine Gland Diseases of Zhejiang Province, 310014 Hangzhou, Zhejiang, China; Clinical Research Center for Cancer of Zhejiang Province, 310014 Hangzhou, Zhejiang, China; [orcid.org/0000-0001-6726-6418](https://orcid.org/0000-0001-6726-6418); Email: [geminghua@hmc.edu.cn](mailto:geminghua@hmc.edu.cn)

**Guowan Zheng** – Otolaryngology & Head and Neck Center, Cancer Center, Department of Head and Neck Surgery, Zhejiang Provincial People's Hospital, Affiliated People's Hospital, Hangzhou Medical College, 310014 Hangzhou, Zhejiang, China; Key Laboratory of Endocrine Gland Diseases of Zhejiang Province, 310014 Hangzhou, Zhejiang, China; Clinical Research Center for Cancer of Zhejiang



Province, 310014 Hangzhou, Zhejiang, China; [orcid.org/0000-0001-5731-8325](https://orcid.org/0000-0001-5731-8325); Email: zhengguowan@hmc.edu.cn

## Authors

**Lei Zhu** – Suzhou Medical College of Soochow University, 215123 Suzhou, Jiangsu, China; Department of Head and Neck Surgery, the Fifth Hospital Affiliated to Wenzhou Medical University, Lishui Central Hospital, 323020 Lishui City, Zhejiang Province, China; Key Laboratory of Endocrine Gland Diseases of Zhejiang Province, 310014 Hangzhou, Zhejiang, China; Clinical Research Center for Cancer of Zhejiang Province, 310014 Hangzhou, Zhejiang, China; [orcid.org/0000-0002-5996-4854](https://orcid.org/0000-0002-5996-4854)

**Ruimin Liang** – Otolaryngology & Head and Neck Center, Cancer Center, Department of Head and Neck Surgery, Zhejiang Provincial People's Hospital, Affiliated People's Hospital, Hangzhou Medical College, 310014 Hangzhou, Zhejiang, China; Key Laboratory of Endocrine Gland Diseases of Zhejiang Province, 310014 Hangzhou, Zhejiang, China; Clinical Research Center for Cancer of Zhejiang Province, 310014 Hangzhou, Zhejiang, China

**Yawen Guo** – Otolaryngology & Head and Neck Center, Cancer Center, Department of Head and Neck Surgery, Zhejiang Provincial People's Hospital, Affiliated People's Hospital, Hangzhou Medical College, 310014 Hangzhou, Zhejiang, China; Key Laboratory of Endocrine Gland Diseases of Zhejiang Province, 310014 Hangzhou, Zhejiang, China; Clinical Research Center for Cancer of Zhejiang Province, 310014 Hangzhou, Zhejiang, China

**Yefeng Cai** – Key Laboratory of Endocrine Gland Diseases of Zhejiang Province, 310014 Hangzhou, Zhejiang, China; Clinical Research Center for Cancer of Zhejiang Province, 310014 Hangzhou, Zhejiang, China; Department of Thyroid Surgery, The First Affiliated Hospital of Wenzhou Medical University, 325015 Wenzhou City, Zhejiang Province, China

**Fahuan Song** – Otolaryngology & Head and Neck Center, Cancer Center, Department of Head and Neck Surgery, Zhejiang Provincial People's Hospital, Affiliated People's Hospital, Hangzhou Medical College, 310014 Hangzhou, Zhejiang, China; Key Laboratory of Endocrine Gland Diseases of Zhejiang Province, 310014 Hangzhou, Zhejiang, China; Clinical Research Center for Cancer of Zhejiang Province, 310014 Hangzhou, Zhejiang, China

**Yiqun Hu** – Otolaryngology & Head and Neck Center, Cancer Center, Department of Head and Neck Surgery, Zhejiang Provincial People's Hospital, Affiliated People's Hospital, Hangzhou Medical College, 310014 Hangzhou, Zhejiang, China; Key Laboratory of Endocrine Gland Diseases of Zhejiang Province, 310014 Hangzhou, Zhejiang, China; Clinical Research Center for Cancer of Zhejiang Province, 310014 Hangzhou, Zhejiang, China

**Yunye Liu** – Otolaryngology & Head and Neck Center, Cancer Center, Department of Head and Neck Surgery, Zhejiang Provincial People's Hospital, Affiliated People's Hospital, Hangzhou Medical College, 310014 Hangzhou, Zhejiang, China; Key Laboratory of Endocrine Gland Diseases of Zhejiang Province, 310014 Hangzhou, Zhejiang, China; Clinical Research Center for Cancer of Zhejiang Province, 310014 Hangzhou, Zhejiang, China

Complete contact information is available at:  
<https://pubs.acs.org/10.1021/acsomega.4c00373>

## Author Contributions

L.Z., R.L., and Y.G. contributed equally to this work. Lei Zhu proposed the ideas, designed the experiments, and wrote the manuscript. Ruimin Liang, Yawen Guo, and Yefeng Cai conducted the experiments; Fahuan Song and Yiqun Hu analyzed the data. Guowan Zheng and Minghua Ge revised the whole manuscript.

## Funding

This study was supported by Lishui Municipal Science and Technology Program (grant no. 2023GYX05), Zhejiang Provincial Natural Science Foundation of China (grant no. LTGY24H070004), the Medical and Health Research Program of Zhejiang Province (grant no. 2023KY420), Zhejiang Provincial Project of Administration of Chinese Medicine (grant nos. 2023ZL240, 2024ZL1292, 2024ZL611, 2024ZL610 and 2024ZL246), National Natural Science Foundation of China (grant no. 82001862), and China Postdoctoral Science Foundation (grant no. 2021M702908).

## Notes

The authors declare no competing financial interest. Ethical Approval: Ethical approval was not required for the study. All public data sets used in this study were obtained from others with ethical approval.

## ACKNOWLEDGMENTS

We thank Home for Researchers editorial team (<https://www.home-for-researchers.com/#/>) for language editing service.

## ABBREVIATIONS

ATC, anaplastic thyroid cancer; TCM, Traditional Chinese medicine; TCMSP, Traditional Chinese Medicine System Pharmacology Database and Analysis Platform; GEO, Gene Expression Omnibus; PPI, protein–protein interaction; GO, gene ontology; KEGG, Kyoto Encyclopedia of Genes and Genomes

## REFERENCES

- (1) Kim, J.; Gosnell, J. E.; Roman, S. A. Geographic influences in the global rise of thyroid cancer. *Nat. Rev. Endocrinol.* **2020**, *16* (1), 17–29.
- (2) Perrier, N. D.; Brierley, J. D.; Tuttle, R. M. Differentiated and anaplastic thyroid carcinoma: Major changes in the American Joint Committee on Cancer eighth edition cancer staging manual. *Ca-Cancer J. Clin.* **2018**, *68* (1), 55–63.
- (3) Lin, B.; Ma, H.; Ma, M.; Zhang, Z.; Sun, Z.; Hsieh, I. Y.; Okenwa, O.; Guan, H.; Li, J.; Lv, W. The incidence and survival analysis for anaplastic thyroid cancer: a SEER database analysis. *Am. J. Transl. Res.* **2019**, *11* (9), 5888–5896.
- (4) Weinberger, P.; Ponny, S. R.; Xu, H.; Bai, S.; Smallridge, R.; Copland, J.; Sharma, A. Cell Cycle M-Phase Genes Are Highly Upregulated in Anaplastic Thyroid Carcinoma. *Thyroid* **2017**, *27* (2), 236–252.
- (5) Li, W.; Li, Y.; Li, J.; Pang, H. Combination of Novel Therapies and New Attempts in Anaplastic Thyroid Cancer. *Technol. Cancer Res. Treat.* **2023**, *22*, 153303382311698.
- (6) Califano, L.; Smulever, A.; Jerkovich, F.; Pitoia, F. Advances in the management of anaplastic thyroid carcinoma: transforming a life-threatening condition into a potentially treatable disease. *Rev. Endocr. Metab. Disord.* **2024**, *25* (1), 123–147.
- (7) Hu, Y.; Wen, Q.; Cai, Y.; Liu, Y.; Ma, W.; Li, Q.; Song, F.; Guo, Y.; Zhu, L.; Ge, J.; Zeng, Q.; Wang, J.; Yin, C.; Zheng, G.; Ge, M. Alantolactone induces concurrent apoptosis and GSDME-dependent pyroptosis of anaplastic thyroid cancer through ROS mitochondria-dependent caspase pathway. *Phytomedicine* **2023**, *108*, 154528.

- (8) Li, L.; Wang, X.; Sharvan, R.; Gao, J.; Qu, S. Berberine could inhibit thyroid carcinoma cells by inducing mitochondrial apoptosis, G0/G1 cell cycle arrest and suppressing migration via PI3K-AKT and MAPK signaling pathways. *Biomed. Pharmacother.* **2017**, *95*, 1225–1231.
- (9) Zhang, C.; Yang, H. Y.; Gao, L.; Bai, M. Z.; Fu, W. K.; Huang, C. F.; Mi, N. N.; Ma, H. D.; Lu, Y. W.; Jiang, N. Z.; Tian, L.; Cai, T.; Lin, Y. Y.; Zheng, X. X.; Gao, K.; Chen, J. J.; Meng, W. B. Lanatoside C decelerates proliferation and induces apoptosis through inhibition of STAT3 and ROS-mediated mitochondrial membrane potential transformation in cholangiocarcinoma. *Front. Pharmacol.* **2023**, *14*, 1098915.
- (10) Ha, D. P.; Tsai, Y. L.; Lee, A. S. Suppression of ER-stress induction of GRP78 as an anti-neoplastic mechanism of the cardiac glycoside Lanatoside C in pancreatic cancer: Lanatoside C suppresses GRP78 stress induction. *Neoplasia* **2021**, *23* (12), 1213–1226.
- (11) Duan, Y.; Chen, L.; Shao, J.; Jiang, C.; Zhao, Y.; Li, Y.; Ke, H.; Zhang, R.; Zhu, J.; Yu, M. Lanatoside C inhibits human cervical cancer cell proliferation and induces cell apoptosis by a reduction of the JAK2/STAT6/SOCS2 signaling pathway. *Oncol. Lett.* **2021**, *22* (4), 740.
- (12) Xu, Y.; Xu, M.; Tong, J.; Tang, X.; Chen, J.; Chen, X.; Zhang, Z.; Cao, B.; Stewart, A. K.; Moran, M. F.; Wu, D.; Mao, X. Targeting the Otub1/c-Maf axis for the treatment of multiple myeloma. *Blood* **2021**, *137* (11), 1478–1490.
- (13) Wang, Y.; Hou, Y.; Hou, L.; Wang, W.; Li, K.; Zhang, Z.; Du, B.; Kong, D. Digoxin exerts anticancer activity on human nonsmall cell lung cancer cells by blocking PI3K/Akt pathway. *Biosci. Rep.* **2021**, *41* (10), BSR20211056.
- (14) Bisht, A.; Tewari, D.; Kumar, S.; Chandra, S. Network pharmacology, molecular docking, and molecular dynamics simulation to elucidate the mechanism of anti-aging action of *Tinospora cordifolia*. *Mol. Diversity* **2023**, *7*, 13.
- (15) Wang, Z.; Xie, X.; Wang, M.; Ding, M.; Gu, S.; Xing, X.; Sun, X. Analysis of common and characteristic actions of *Panax ginseng* and *Panax notoginseng* in wound healing based on network pharmacology and meta-analysis. *J. Ginseng Res.* **2023**, *47* (4), 493–505.
- (16) Li, X.; Liu, Z.; Liao, J.; Chen, Q.; Lu, X.; Fan, X. Network pharmacology approaches for research of Traditional Chinese Medicines. *Chin. J. Nat. Med.* **2023**, *21* (5), 323–332.
- (17) Li, S. Exploring traditional chinese medicine by a novel therapeutic concept of network target. *Chin. J. Integr. Med.* **2016**, *22* (9), 647–652.
- (18) Ru, J.; Li, P.; Wang, J.; Zhou, W.; Li, B.; Huang, C.; Li, P.; Guo, Z.; Tao, W.; Yang, Y.; Xu, X.; Li, Y.; Wang, Y.; Yang, L. TCMSP: a database of systems pharmacology for drug discovery from herbal medicines. *J. Cheminf.* **2014**, *6*, 13.
- (19) Chen, F.; Chai, Y. H.; Zhang, F.; Liu, Y. Q.; Zhang, Y.; Shi, Y. J.; Zhang, J. M.; Leng, Y. F. Network pharmacology analysis combined with experimental validation to explore the therapeutic mechanism of salidroside on intestine ischemia reperfusion. *Biosci. Rep.* **2023**, *43* (8), BSR20230539.
- (20) Ji, L.; Song, T.; Ge, C.; Wu, Q.; Ma, L.; Chen, X.; Chen, T.; Chen, Q.; Chen, Z.; Chen, W. Identification of bioactive compounds and potential mechanisms of *scutellariae radix-coptidis rhizoma* in the treatment of atherosclerosis by integrating network pharmacology and experimental validation. *Biomed. Pharmacother.* **2023**, *165*, 115210.
- (21) Li, G.; Wang, Q.; Chen, X.; Yu, P.; Peng, Q.; Chen, H.; Ren, S.; Wang, C.; Su, Y.; Liang, X.; Sun, M.; Du, X.; He, R. Based on network pharmacology to explore the effect and mechanism of Yipibushen decoction in improving obese type 2 diabetes mellitus with oligoaesthenospermia. *J. Ethnopharmacol.* **2023**, *317*, 116738.
- (22) Bateman, A.; Martin, M. J.; Orchard, S.; Magrane, M.; Agivetova, R.; Ahmad, S.; Alpi, E.; Bowler-Barnett, E. H.; Britto, R.; Bursteinas, B.; et al. UniProt: the universal protein knowledgebase in 2021. *Nucleic Acids Res.* **2021**, *49* (D1), D480–D489.
- (23) Lu, S.; Sun, X.; Zhou, Z.; Tang, H.; Xiao, R.; Lv, Q.; Wang, B.; Qu, J.; Yu, J.; Sun, F.; Deng, Z.; Tian, Y.; Li, C.; Yang, Z.; Yang, P.; Rao, B. Mechanism of Bazhen decoction in the treatment of colorectal cancer based on network pharmacology, molecular docking, and experimental validation. *Front. Immunol.* **2023**, *14*, 1235575.
- (24) Xiaoying, M.; Zhiming, H.; Tao, Y.; Jun, X.; Ying, Z.; Na, G.; Xun, C.; Guoli, L.; Hong, W. Elucidating the molecular mechanisms underlying anti-inflammatory effects of *Morchella esculenta* in the arachidonic acid metabolic pathway by network pharmacology and molecular docking. *Sci. Rep.* **2023**, *13* (1), 15881.
- (25) Jia, F.; Chen, Y.; Xin, G.; Li, L.; Liu, Z.; Xu, S.; Gao, J.; Meng, H.; Shi, Y.; Ma, Y.; Li, L.; Fu, J. Shuangshen Ningxin capsule alleviates myocardial ischemia-reperfusion injury in miniature pigs by modulating mitophagy: network pharmacology and experiments in vivo. *China's Med.* **2023**, *18* (1), 120.
- (26) Huagang, H.; Ziqiang, L. L.; Jingfeng, O.; Tianquan, W.; Lingyan, D.; Junling, C. Mechanism of Lingbao Huxin Dan in the treatment of bradyarrhythmia complicated with coronary heart disease: a network pharmacology analysis. *J. Tradit. Chin. Med. Sci.* **2023**, *43* (5), 1001–1009.
- (27) Ren, T.; Yin, N.; Du, L.; Pan, M.; Ding, L. Identification and validation of FPR1, FPR2, IL17RA and TLR7 as immunogenic cell death related genes in osteoarthritis. *Sci. Rep.* **2023**, *13* (1), 16872.
- (28) Shi, Y.; Wang, Y.; Dong, H.; Niu, K.; Zhang, W.; Feng, K.; Yang, R.; Zhang, Y. Crosstalk of ferroptosis regulators and tumor immunity in pancreatic adenocarcinoma: novel perspective to mRNA vaccines and personalized immunotherapy. *Apoptosis* **2023**, *28* (9–10), 1423–1435.
- (29) Deng, J.; Qin, L.; Zhou, Z. Network Pharmacology and Molecular Docking Reveal the Mechanism of *Isodon ternifolius* (D. Don) Kudo Against Liver Fibrosis. *Drug Des., Dev. Ther.* **2023**, *17*, 2335–2351.
- (30) Szklarczyk, D.; Gable, A. L.; Nastou, K. C.; Lyon, D.; Kirsch, R.; Pyysalo, S.; Doncheva, N. T.; Legeay, M.; Fang, T.; Bork, P.; Jensen, L. J.; von Mering, C.; Mering, C. Correction to 'The STRING database in 2021: customizable protein-protein networks, and functional characterization of user-uploaded gene/measurement sets'. *Nucleic Acids Res.* **2021**, *49* (18), 10800.
- (31) Zhang, X. L.; Zhang, X. F.; Fang, Y.; Li, M. L.; Shu, R.; Gong, Y.; Luo, H. Y.; Tian, Y. A possible genetic association between obesity and colon cancer in females. *Front. Endocrinol.* **2023**, *14*, 1189570.
- (32) Liu, M.; Huang, L.; Liu, Y.; Yang, S.; Rao, Y.; Chen, X.; Nie, M.; Liu, X. Identification of the MMP family as therapeutic targets and prognostic biomarkers in the microenvironment of head and neck squamous cell carcinoma. *J. Transl. Med.* **2023**, *21* (1), 208.
- (33) Smach, M. A.; Hafsa, J.; Ben Abdallah, J.; Charfeddine, B.; Limem, K. Neuroprotective and anti-amnesic effects of *Laurus Nobilis* essential oil against scopolamine-induced memory deficits in mice brain. *J. Ethnopharmacol.* **2024**, *319* (Pt 1), 117151.
- (34) Ran, R.; Tu, G.; Li, H.; Wang, H.; Mou, E.; Liu, C. Genetic Variants Associated with Thyroid Cancer Risk: Comprehensive Research Synopsis, Meta-Analysis, and Cumulative Epidemiological Evidence. *J. Oncol.* **2021**, *2021*, 1–11.
- (35) Abutorabi, E. S.; Poursheikhani, A.; Kashani, B.; Shamsaiegahkani, S.; Haghpanah, V.; Bashash, D.; Mousavi, S. A.; Momeny, M.; Ghaffari, S. H. The effects of Abemaciclib on cell cycle and apoptosis regulation in anaplastic thyroid cancer cells. *Mol. Biol. Rep.* **2023**, *50* (5), 4073–4082.
- (36) Rao, S. N.; Smallridge, R. C. Anaplastic thyroid cancer: An update. *Best Pract. Res. Clin. Endocrinol. Metab.* **2023**, *37* (1), 101678.
- (37) Zhang, L.; Feng, Q.; Wang, J.; Tan, Z.; Li, Q.; Ge, M. Molecular basis and targeted therapy in thyroid cancer: Progress and opportunities. *Biochim. Biophys. Acta, Rev. Cancer* **2023**, *1878* (4), 188928.
- (38) Iesato, A.; Li, S.; Sadow, P. M.; Abbasian, M.; Nazarian, A.; Lawler, J.; Nucera, C. The Tyrosine Kinase Inhibitor Lenvatinib Inhibits Anaplastic Thyroid Carcinoma Growth by Targeting Pericytes in the Tumor Microenvironment. *Thyroid* **2023**, *33* (7), 835–848.
- (39) Gao, X.; Hong, C.; Xie, Y.; Zeng, X. Immunotherapy or targeted therapy: What will be the future treatment for anaplastic thyroid carcinoma? *Front. Oncol.* **2023**, *13*, 1103147.

- (40) Uppalapati, S. S.; Guha, L.; Kumar, H.; Mandoli, A. Nanotechnological Advancements For The Theranostic Intervention In Anaplastic Thyroid Cancer: Current Perspectives And Future Direction. *Curr. Cancer Drug Targets* **2023**, *24*, 245.
- (41) Park, B. H.; Jung, K. H.; Son, M. K.; Seo, J. H.; Lee, H. S.; Lee, J. H.; Hong, S. S. Antitumor activity of Pulsatilla koreana extract in anaplastic thyroid cancer via apoptosis and anti-angiogenesis. *Mol. Med. Rep.* **2013**, *7* (1), 26–30.
- (42) Chakraborty, J.; Chakraborty, S.; Chakraborty, S.; Narayan, M. N. Entanglement of MAPK pathways with gene expression and its omnipresence in the etiology for cancer and neurodegenerative disorders. *Biochim. Biophys. Acta, Gene Regul. Mech.* **2023**, *1866* (4), 194988.
- (43) Huang, Y.; Zhen, Y.; Chen, Y.; Sui, S.; Zhang, L. Unraveling the interplay between RAS/RAF/MEK/ERK signaling pathway and autophagy in cancer: From molecular mechanisms to targeted therapy. *Biochem. Pharmacol.* **2023**, *217*, 115842.
- (44) Fagin, J. A.; Krishnamoorthy, G. P.; Landa, I. Pathogenesis of cancers derived from thyroid follicular cells. *Nat. Rev. Cancer* **2023**, *23* (9), 631–650.
- (45) Leandro-García, L. J.; Landa, I. Mechanistic Insights of Thyroid Cancer Progression. *Endocrinology* **2023**, *164* (9), bqad118.
- (46) Fu, H.; Cheng, L.; Jin, Y.; Cheng, L.; Liu, M.; Chen, L. MAPK Inhibitors Enhance HDAC Inhibitor-Induced Redifferentiation in Papillary Thyroid Cancer Cells Harboring BRAF (V600E): An In Vitro Study. *Mol. Ther.—Oncolytics* **2019**, *12*, 235–245.
- (47) Cabanillas, M. E.; Ryder, M.; Jimenez, C. Targeted Therapy for Advanced Thyroid Cancer: Kinase Inhibitors and Beyond. *Endocr. Rev.* **2019**, *40* (6), 1573–1604.
- (48) Eberhardt, J.; Santos-Martins, D.; Tillack, A. F.; Forli, S. AutoDock Vina 1.2.0: New Docking Methods, Expanded Force Field, and Python Bindings. *J. Chem. Inf. Model.* **2021**, *61* (8), 3891–3898.
- (49) Trott, O.; Olson, A. J. AutoDock Vina: improving the speed and accuracy of docking with a new scoring function, efficient optimization, and multithreading. *J. Comput. Chem.* **2010**, *31* (2), 455–461.
- (50) Liu, J.; Li, S. M.; Tang, Y. J.; Cao, J. L.; Hou, W. S.; Wang, A. Q.; Wang, C.; Jin, C. H. Jaceosidin induces apoptosis and inhibits migration in AGS gastric cancer cells by regulating ROS-mediated signaling pathways. *Redox Rep.* **2024**, *29* (1), 2313366.
- (51) Guo, Q. R.; Zhou, W. M.; Zhang, G. B.; Deng, Z. F.; Chen, X. Z.; Sun, F. Y.; Lei, X. P.; Yan, Y. Y.; Zhang, J. Y. Jaceosidin inhibits the progression and metastasis of NSCLC by regulating miR-34c-3p/Integrin  $\alpha2\beta1$  axis. *Heliyon* **2023**, *9* (5), No. e16158.
- (52) Shi, M.; Chen, Z.; Gong, H.; Peng, Z.; Sun, Q.; Luo, K.; Wu, B.; Wen, C.; Lin, W. Luteolin, a flavone ingredient: Anticancer mechanisms, combined medication strategy, pharmacokinetics, clinical trials, and pharmaceutical researches. *Phytother. Res.* **2024**, *38* (2), 880–911.
- (53) Liu, B.; Zhao, X.; Zhang, S.; Li, Q.; Li, X.; Huang, D.; Xia, J.; Ma, N.; Duan, Y.; Zhang, X.; Rao, J. Targeting ZDHHC21/FASN axis for the treatment of diffuse large B-cell lymphoma. *Leukemia* **2024**, *38* (2), 351–364.
- (54) Hou, Y. Q.; Wang, Y. Y.; Wang, X. C.; Liu, Y.; Zhang, C. Z.; Chen, Z. S.; Zhang, Z.; Wang, W.; Kong, D. X. Multifaceted anti-colorectal tumor effect of digoxin on HCT8 and SW620 cells in vitro. *Gastroenterol. Rep.* **2020**, *8* (6), 465–475.
- (55) Kong, P.; Tang, X.; Liu, F.; Tang, X. Astragaloside IV regulates circ\_0001615 and miR-873-5p/LASP1 axis to suppress colorectal cancer cell progression. *Chem. Biol. Drug Des.* **2024**, *103* (1), No. e14423.
- (56) Shen, L.; Li, Y.; Hu, G.; Song, X.; Wang, X.; Li, X.; Xu, X. Astragaloside IV suppresses the migration and EMT progression of cervical cancer cells by inhibiting macrophage M2 polarization through TGF $\beta$ /Smad2/3 signaling. *Funct. Integr. Genomics* **2023**, *23* (2), 133.
- (57) Lindholm, H.; Ejeskär, K.; Szekeres, F. Digitoxin Affects Metabolism, ROS Production and Proliferation in Pancreatic Cancer Cells Differently Depending on the Cell Phenotype. *Int. J. Mol. Sci.* **2022**, *23* (15), 8237.
- (58) Mi, C.; Cao, X.; Ma, K.; Wei, M.; Xu, W.; Lin, Y.; Zhang, J.; Wang, T. Y. Digitoxin promotes apoptosis and inhibits proliferation and migration by reducing HIF-1 $\alpha$  and STAT3 in KRAS mutant human colon cancer cells. *Chem.-Biol. Interact.* **2022**, *351*, 109729.